Scripta Materialia 124 (2016) 174–178

Contents lists available at ScienceDirect

Scripta Materialia

journal homepage: www.elsevier.com/locate/scriptamat

Regular Article

Multivariate-aided mapping of rare-earth partitioning in a wrought magnesium alloy

David Rossouw [a,*], Brian Langelier [a], Andrew Scullion [a], Mohsen Danaie [b], Gianluigi A. Botton [a]

[a] Department of Materials Science and Engineering, McMaster University, 1280 Main Street West, Hamilton, Ontario, L8S 4L7, Canada
[b] Department of Materials, University of Oxford, 16 Parks Road, Oxford OX1 3PH, UK

ARTICLE INFO

Article history:
Received 12 April 2016
Received in revised form 12 July 2016
Accepted 14 July 2016
Available online xxxx

Keywords:
Rare earth
Magnesium alloys
Transmission electron microscopy (TEM)
Electron energy loss spectroscopy (EELS)
Multivariate statistical analysis

ABSTRACT

The formability of wrought magnesium alloys can be dramatically improved by the addition of trace rare-earth elements, which can weaken the recrystallized texture. Improving the understanding of this texture-weakening mechanism requires knowledge of the precise location of the solute species in the microstructure. Here we study the partitioning of the trace alloying elements in a rare-earth magnesium alloy using analytical electron microscopy and atom probe tomography, combined with multivariate statistical methods. The analysis reveals partitioning of solutes to grain boundaries and precipitate-matrix interfaces.

1. Main body

The widespread use of wrought magnesium for rolled sheet products has been limited by its inherently poor formability [1]. Several alloying additions, including Li, Ca and a range of rare-earth (RE) metals, have been shown to be effective in reducing magnesium's strong basal texture, thereby improving formability [2]. While the favorable texture weakening effect of RE alloying has been known for decades [3], a fundamental understanding of the mechanism behind RE texturing is still subject to debate [4]. A necessary pre-requisite to an improved understanding of the texture-weakening mechanism demands knowledge of the precise location of the solute species in the microstructure. Relatively few comprehensive high-resolution analytical transmission electron microscopy (TEM) studies have been conducted on the analysis of solute segregation in dilute Mg-RE alloys. Among these, the high angle annular dark field scanning transmission electron microscopy (HAADF-STEM) technique has proven valuable in the characterization of precipitates [5], grain boundary segregation [6,7], twin boundary segregation [8] and even single atom dopant detection [7,9]. HAADF-STEM has also played a central role in the study of precipitation sequences in dilute magnesium rare-earth alloys during the early stages of aging [10,11].

In this study, we employ advanced analytical TEM techniques and 3D atom probe tomography (APT) to study the microstructure and distribution of trace solute elements in a commercial ZEK100 magnesium sheet alloy. The ZEK100 series, containing Nd, Zn and Zr, has been developed for wrought sheet product applications where superior formability is paramount [12]. Zn can be used to improve the alloy's strength and creep resistance [13], and Zr may be added to refine the grain size and improve the corrosion resistance of the alloy [14]. The alloy studied was hot rolled to 1.5 mm thickness and annealed after processing to soften it prior to forming. A 3 mm disk was cut from a formed sheet and thinned to electron transparency using an Allied High Tech MultiPrep polishing machine, followed by gentle ion milling using a Gatan PIPS machine to remove the surface oxide layer. The nominal composition of the alloy is summarized in Table 1.

Electron micrographs of the alloy were obtained using an aberration corrected FEI Titan 80–300 cubed TEM operated in scanning transmission mode at 300 kV. Fig. 1(a) displays a HAADF-STEM image of a thin area of the specimen selected for electron energy loss spectroscopy (EELS) mapping. The element maps of the solute species Nd, Zn, and Zr, extracted by conventional background subtracted edge integration over the energy windows indicated, are shown in Fig. 1(b–d). The region is comprised of Zn + Zr rich elongated precipitates embedded in an Mg matrix and Zn is observed to decorate the grain boundaries. The segregation of Nd is on the limit of detection in these maps, so we now turn to the aid of multivariate statistical methods, namely independent component analysis (ICA) [15,16], to better extract the inherently low signals associated with dilute solute concentrations contained within the EELS dataset.

We turn our attention to a region in the alloy containing a small cluster of precipitates. Fig. 2 displays EELS maps of the distribution of Nd, Zn and Zr in the region in addition to the ICA decomposition of the EELS

* Corresponding author.
E-mail address: rossoud@mcmaster.ca (D. Rossouw).

http://dx.doi.org/10.1016/j.scriptamat.2016.07.022
1359-6462/

Table 1
Nominal composition (wt.%) of the ZEK100 alloy.

	Zn	Zr	Nd	Mn	Ce	La	Mg
wt.%	1.3	0.25	0.20	0.01	<0.01	<0.01	Bal.
at.%	0.49	0.067	0.034	<0.01	<0.01	<0.01	Bal.

dataset. Based on the element maps, Nd appears to surround the Zn + Zr rich precipitates embedded in the magnesium matrix. The first six components of the ICA data decomposition explain over 99.9% (e, insert) of the variance in the dataset and are displayed in Fig. 2(e). Of these components, component IC#4, containing overlapping Nd-M_{45} and Zn-L_{23} edge structures, indicates the possible co-segregation of Nd and Zn in the region. Similarly, component IC#5, containing Zn-L_{23} and Zr-L_{23} edge structures, suggests the possible co-segregation of Zn and Zr. The corresponding spatial loadings of the IC#4 and IC#5 are shown in Fig. 2(f,g). IC#4 appears to map to shell-like structures enclosing the elongated precipitates. IC#5 maps directly to the precipitates in agreement with the EELS maps for Zn and Zr (c,d). If the Zr-L_{23} map is subtracted from Zn-L_{23}, the residual Zn-L_{23} signal appears to occupy a shell structure around the precipitate much like the element map of Nd-M_{45} (Fig. 2h).

Fig. 3 displays a high-resolution HAADF STEM image of an isolated precipitate. By comparing of the local image Fourier transform to simulated diffraction patterns calculated using the JEMS software package [17], the precipitate was identified as a Zn_2Zr_3 tetragonal P42/mnn (136) crystal structure (a = b = 0.7633 nm, c = 0.6965 nm) [18] viewed down the ⟨111⟩ zone axis (Fig. 3a,i). Enlarged views of the precipitate-matrix interface are shown in Fig. 3(b,c). The brighter columns are richer in Zn than the darker columns, as confirmed by HAADF STEM image simulation (Fig. 3b, ii). At the parallel interfaces, the stacking sequence in the [1–10] direction is terminated by two adjacent monolayers containing columns of similar brightness (b,c, indicated by arrows). The reduced brightness of the columns in the outermost layer, compared to those in the equivalent layers within the precipitate (circled yellow in (c)), may be explained by an increased Zn fraction in the outer monolayer. This is consistent with the prior EELS observation of Zn rich precipitate shells. The prior EELS measurements also show that Nd encapsulates the Zn + Zr rich precipitates, but we cannot determine from these high resolution images alone whether Nd co-exists with Zn and Zr at the precipitate-matrix interface. To address this question, and to validate the ICA findings, we turn to APT for its combination of high 3D spatial resolution and elemental sensitivity.

ZEK100 samples for APT experiments were first sharpened by the standard two-stage electro-polishing route [19]. The needle samples were then cleaned of surface oxides and finely-sharpened in a Zeiss NVison 40 scanning electron microscope, equipped with a focused ion beam. Ion milling was performed at an accelerating voltage of 10 kV. A local-electrode atom probe (Cameca LEAP 4000×-HR) was used for APT data acquisition. The sample was held at ~54 K and evaporated in laser pulsing mode (λ = 355 nm) at a 250 kHz frequency and 90 pJ pulse energy, with a target detection rate of 0.03 ions/pulse. Data reconstruction and analysis were performed using IVAS v3.6.6 software, and established reconstruction algorithms. The reconstruction was spatially calibrated by identifying crystal poles in the detector desorption map, and adjusting the reconstruction parameters to achieve plane spacing values at those poles equal to the known plane spacing values for Mg [19,20]. Fig. 4 displays the analysis of a reconstructed volume containing a Zr rich precipitate. The composition of the precipitate is measured to be 62.6 ± 0.3 at.% Zr, 33.2 ± 0.2 at.% Zn, with 2.6 ± 0.1 at.% Al, and 1.5 ± 0.1 at.% Mg, also detected. Close examination of the interface confirms the presence of Nd in a layer surrounding the precipitate. However it is noted that due to local magnification effects, the majority of the Nd appears away from the precipitate, into the Mg matrix (Fig. 4a,c). This is a typical aberration found in APT data of precipitates with a higher evaporation field than the matrix, particularly in directions

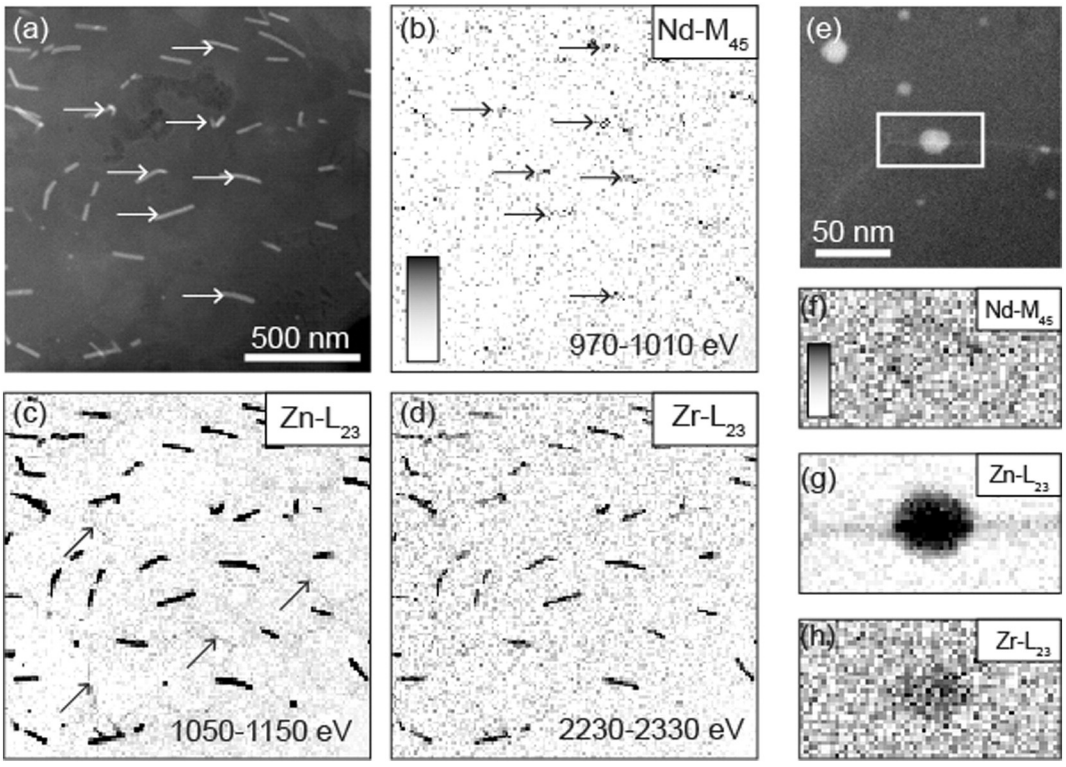

Fig. 1. EELS element mapping of a polycrystalline region containing elongated precipitates. (a) A HAADF-STEM image (arrows pointing to selected precipitates and matched to (b)). Background subtracted element maps of (b) neodymium (arrows pointing to segregation clusters), (c) zinc (arrows pointing to selected grain boundary segregation) and (d) zirconium. (e) EELS element mapping of a round precipitate located on a grain boundary. Background subtracted element maps of (f) neodymium, (g) zinc and (h) zirconium.